Desalination and Water Treatment
www.deswater.com

doi: 10.1080/19443994.2016.1172511

57 (2016) 27152–27168
December

Taylor & Francis
Taylor & Francis Group

Experimental study on the effect of feed water nozzles on non-equilibrium temperature difference and flash evaporation in a single-stage evaporator and an investigation of effect of process parameters on the liquid flashing in a LTTD desalination process

Dilli Balaji

Department of Ocean Structures, National Institute of Ocean Technology, Chennai, India, Tel. +91 44 66783349; Fax: +91 44 66783580; email: dbalaji@niot.res.in

Received 18 September 2015; Accepted 24 March 2016

ABSTRACT

Low temperature thermal desalination (LTTD) process involves flash evaporation of a seawater at 28–29˚C in a single-stage evaporator maintained at a vacuum of around 25–27 m bar (abs). The seawater was splashed inside an evaporator through a 0.1 m diameter upward facing nozzles of around 24 nos arranged evenly throughout the evaporator and generated vapour was condensed in the shell and tube condenser using cooling water available at 12–13˚C sucked from the deep sea through a long HDPE pipe. The main objective of this study was to find out the effect of geometry of the upward facing nozzles on the flash evaporation rate as well as on the non-equilibrium temperature difference (NETD) of the flashing process. Two different spout nozzle geometries with 0.37–0.87 m height were used in the experiment. The study indicated that the flashing rate increased by 0.9% (average) and and the NETD ($T_{wo} - T_{sat}$) decreased by 0.7˚C (average), respectively, when nozzle height was increased by 0.87 m. Mechanism that controlled these two factors were identified and discussed in this paper. Drawbacks of 0.37 m nozzle geometry was also discussed. It was reported in literature that 4% yield ratio was obtained for a nozzle injection pressure of 1 bar for a similar desalination process. But in the present study, a maximum of 1.12% yield ratio was obtained with a nozzle injection pressure of around 0.17 bar. In this work,the effect of the process parameters on the liquid flashing in a LTTD desalination process was investigated and discussed. In order to fine tune the evaporator design for the future LTTD plants, the experimental results of flash evaporation were compared with two mathematical models obtained from the literature. While comparing the results, it was observed that the model which used actual heat ($T_{wi} - T_{wo}$) made a good agreement with the experimental data compared to the other model that used superheat ($T_{wi} - T_{sat}$). From the experimental study, it was observed that the NETD (i.e. thermal loss) measured was found to be higher than the predicted value. The reason that caused the difference in the NETD value was investigated and discussed. Suitable suggestions to reduce these NETD in the flashing process were also presented.

Keywords: Flash evaporation; NETD; Evaporator; Super heat; Actual heat; Flashing efficiency; Evaporation ratio; Feed rate; Feed water nozzle

1. Introduction

Flash evaporation is a phenomenon in which a liquid is exposed suddenly to a low-pressure zone where it undergoes a rapid boiling. In other words, if the pressure acting on the surface of water is suddenly reduced to a pressure far below the saturation pressure of the water corresponding to its temperature then flash evaporation occurs. Increase in super heat result in increase in flash evaporation rate, i.e. when the temperature of feed water increases to a certain degree above the saturation temperature with respect to the saturation pressure maintained in a chamber then flash evaporation take place. This could be due to loss of intermolecular bonding between the molecules by reduction in surface pressure (with respect to ambient pressure) that makes the water molecule to become unstable and free to move from the liquid surface. Presence of salt impurities in the medium such as seawater needs an extra energy to break these molecular bonding that could be achieved either by reducing the surrounding pressure further below the saturation pressure of water corresponding to its saturation temperature or by increasing the temperature of the medium to a point called as boiling point elevation (BPE). Properties of the liquid also play a significant role in the evaporation rate. Degree of superheat available in the liquid corresponding to the saturation pressure actually distinguishes the flash evaporation from the simple evaporation. To attain a thermal equilibrium with the surrounding pressure, the flashed water undergoes a temperature drop when exposed to a sudden vacuum. Flash evaporation may occur violently on the surface and suppress slowly with the increase in water depth. Sensible heat carried by the liquid when exposed to low-pressure zone actually converted in to the latent heat for vaporization. Temperature of liquid exists mainly due to the friction heat generated between the molecules when they were moving randomly in the liquid. Sudden drop in pressure allow these molecules to move out of liquid surface developing a kind of void space temporarily. This event reduce the molecules counting on the water surface that resulted in decrease in the frequency of molecules rubbing with each other, which ultimately produces less heat with reduced liquid temperature. Sub-cooled liquid can be converted to a superheated liquid, when the pressure acting on the liquid surface reduced far below the saturation pressure of the sub-cooled water at that temperature or by increasing the temperature of the sub-cooled liquid to far above the saturation temperature corresponding to saturation pressure maintained on the liquid surface. In simple evaporation, the change in the surface temperature of liquid is believed to be in a linear pattern where as in the flash evaporation a step change in surface temperature occurs which is due to sudden exposure of liquid to a low pressure zone [1].

Miyatake et al. [2] conducted experiments on the spray flash evaporation at an initial temperature of 60℃ and the effect of superheat, spray flow rates and the nozzle diameter on the spray flash evaporation was analysed. From this experiment, it was observed that the flash evaporation rate of jet of liquid was comparably faster than the evaporation rate of flow of super heat liquid as commonly taking place in the conventional multistage evaporators. In the same year, Miyatake et al. [3] presented another paper in which spray flash evaporation was done at two different temperatures of 40–80℃. From this experiment, it was found that even at less temperature of feed water, spray flash evaporation had a faster evaporation rate and higher rate of evaporation than the normal process occurring in evaporators such as MSF. Kitamura et al. [4] studied the critical superheat for flashing of jet of liquids such as water and ethanol into the vacuum chamber through a long nozzle. During this work, two types of patterns were observed in the flashing jet one was complete flashing and other one was two-phase vapour–liquid effluent. It was reported that complete flashing occurs if the temperature of jet of water increases well above the saturation temperature of water corresponding to that chamber pressure. Gopalakrishna et al. [5] conducted experiments using fresh water and also with sodium chloride (NaCl) solution in a cylindrical vessel of diameter 152 mm at varying water depths of 165,305, and 457 mm at initial temperatures of 25–80℃ with initial superheats of 0.5–10℃. It was observed during the experiment that as the evaporation undergoes, the temperature of the water dropped gradually to an equilibrium value corresponding to the final pressure. They suggested dimensionless parameters, which controls rate of evaporation in pools, are Jakob number, Prandtl number, hydrostatic head and salt concentration. To predict the evaporation rate and non-equilibrium fraction (NEF) Miyatake et al. [6] proposed a correlation $\mathrm{NEF} = T(t) - T_e/T_i - T_e$, which consist of dimensional parameters such as T_i initial bulk average temperature of the water, prior to flashing, $T(t)$ is the bulk-average temperature of the water at time t after flashing commenced and T_e is the equilibrium temperature after flashing practically ceased. They conducted experiments at 100 mm shallower water depth and 200 mm deeper water depth and found that lower depth and high initial temperature of water has lower tendency to suppress the nucleation of bubble as well as its growth. In lower depths of pool, large size bubbles

were forming and as it rises to the top, it collapses resultant in the decrease of the bulk pool temperature, which leads to diminished evaporation rate. Ikegami et al. [7] showed in their experiment that, the evaporation rate is faster in the vertical upward flow jets rather than the downward flow jets. Brown and York [8] conducted experiments by flashing liquid jets using rough orifices and sharp edge orifices. They concluded that the liquid jet was shattered by rapid bubble growth and also stated that weber number and degree of superheat controlled the rapid bubble growth. Muthunayagam et al. [9] conducted experiment using saline water at temperatures between 26 and 32°C in a pilot model plant between the operating pressures of 13–23 m bar. Through pilot model they demonstrated the feasibility of the devising a desalination system using difference in ocean temperatures. They obtained a yield up to 4% as estimated by the theoretical model developed for this work. A swirl injection nozzle used for spraying water in garden was utilised for the experiment with an injection pressure of about 1 bar sufficient for achieving the necessary evaporation.

Direct comparison of the present work objective with other works would be a challenging task. Since the literature survey revealed that most of the works related to the flash evaporation were performed in a controlled environment with a small to medium-sized experimental set-up, whereas in the present work, the experiments were conducted and data were recorded in a real time from a running plant of 100 m^3/d capacity where the operating parameters such as cooling water temperature, feed water inlet temperature, mass flow rate of feed and cooling water were subjected to dynamic conditions as a result of tidal variation and ocean currents. However, an attempt had been made to compare the present work objective with the other author's work wherever possible and presented in this paper. In the current work, the effect of two different feed water nozzles geometry on the flashing process as well as thermal losses, i.e. NETD ($T_{wo} - T_{sat}$) were studied. Experiments were carried out with two different spout nozzles of 0.37 m (Fig. 1) and 0.87 m (Fig. 2) height. Results of the study indicated that the flash evaporation rate was increased by 0.9% average and the NETD was decreased by 0.7°C average, respectively, when nozzle height was increased from 0.37 to 0.87 m. Mechanism that controlled these two factors were identified and discussed in this paper. Limitations of 0.37 m nozzle geometry on the evaporation rate and NETD were also discussed. In order to improve the evaporator design for the future low temperature thermal desalination (LTTD) plants, the experimental results of flash evaporation were compared with two mathematical models obtained from the literature. While comparing the results, it was observed that the model which used actual heat ($T_{wi} - T_{wo}$) made a good agreement with the experimental data compared to the other model that used

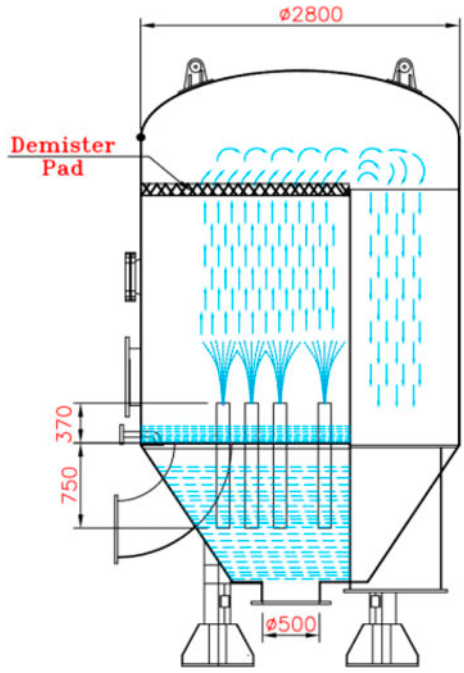

Fig. 1. Evaporator with 0.37 m height nozzle.

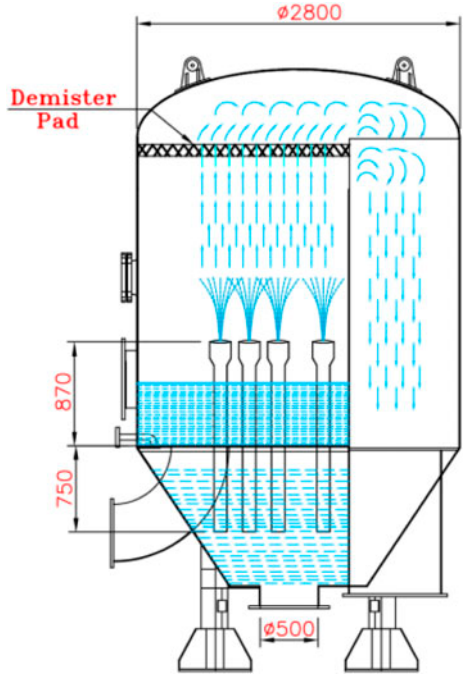

Fig. 2. Evaporator with 0.87 m height nozzle.

superheat ($T_{wi} - T_{sat}$). Where T_{wi}, T_{wo}, and T_{sat} are feed water inlet, outlet temperature and saturation temperature, respectively. From the experimental study, it was observed that the NETD (i.e. thermal loss) measured was found to be greater than the predicted value. Reasons for the variation in the measured NETD value with the predicted one was investigated and discussed in this paper. Suitable suggestions to reduce these NETD in the LTTD flashing process were also presented in this work. This paper discussed about the effect of tidal level variation on the flashing process. Apart from that, an investigation of the effect of process parameters on the liquid flashing for 0.87 m nozzle configuration was also carried out and the results were discussed in this paper. Schematic of LTTD process is shown in Fig. 3. During the experiment, it was observed that the temperature of the warm surface seawater varied from 28.3 to 29.9˚C and showed an increasing trend with the warm water feed rate. This could be due to seasonal variations in the sea state. Experiment was conducted in a single-stage cylindrical flash evaporator of 2.8 m diameter and 4.5 m tall. This evaporator was fabricated with inbuilt de-aerator of conical truncated shape provided at the bottom of the evaporator. Warm feed water enters the de-aerator initially, where the non-condensable gases present in the seawater were removed and then the feed water enters the evaporator through upward facing spout nozzles with quantity of around 24 nos evenly distributed inside the evaporator. Spout nozzle serve two purposes one for enhancing the evaporation rate and another one to maintain differential pressure between the evaporator and the de-aerator that varied between 120 and 200 m bar observed during the experiment.

2. Experimental Set-up

The experiments have been conducted in the running plant located at Minicoy in UT Lakshadweep group of Islands. A single-stage evaporator was used in the plant (Fig. 4) for generating water vapour under low vacuum of around 24–27 m bar (abs). The evaporator is made up of SS 304 material. It is located at an elevation of around + 10.8 m from the mean sea level. Since no brine discharge pump was used, maintaining the barometric height becomes very essential to discharge out the brine water. Two different geometry spout nozzles were used in the experiment. These nozzles were arranged evenly and fixed with the bottom plate of the evaporator, which actually divides the evaporator compartment from the de-aerator tank located below. The pressure maintained inside the chamber was measured by using two vacuum transmitters; one is located at the side wall of the evaporator at height of around 1.2 m from the base and another one at the top dome of the evaporator. The accuracy of the vacuum transmitter is around ±0.01 m bar. Level indicator was mounted on the evaporator shell to monitor the water level that is subjected to variation depending upon the changes in the tide level. The flow rate of the warm feed water was measured using the insertion-type flow metre of E + H make with an accuracy of ±1 kg/s. The flow metre

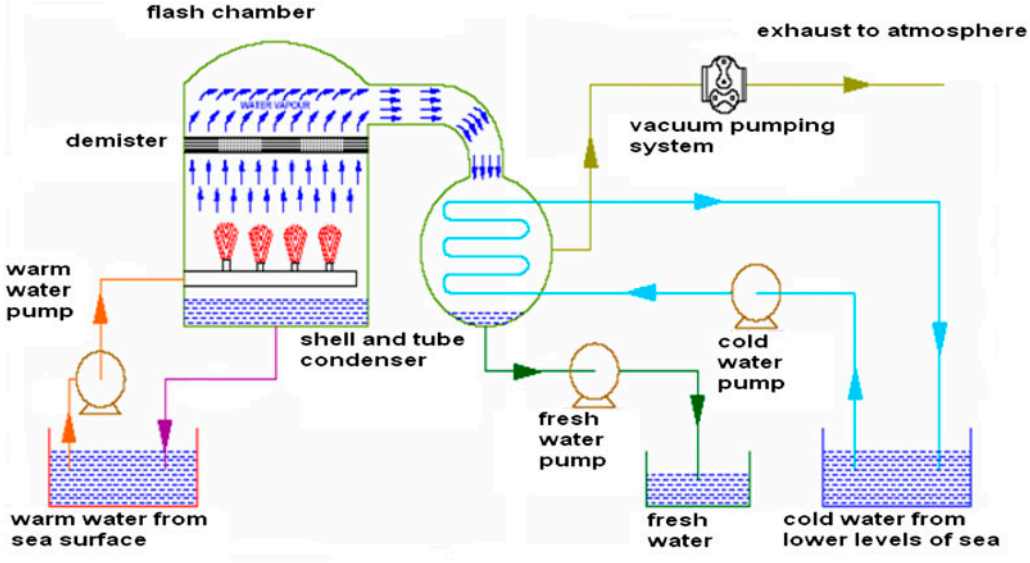

Fig. 3. Schematic view of LTTD plant.

Fig. 4. View of single-stage evaporator.

was installed in the 0.57 m diameter pipeline in the upstream side of the evaporator. For measuring the flow rate of the condensed freshwater from the surface condenser, in-line magnetic flow metre was used. The accuracy of this flow metre is around ±1 kg/s, which is of Honey-well make. Similarly, to measure the temperature of the inlet warm feed water and brine discharge water, temperature transmitters were used. The accuracy of the temperature transmitter is around ±0.01˚C (Make: Honey-well). 450 NB butterfly valves were being used for regulating the flow rate of the feed water. Submersible type seawater pump (Make: Wilo pumps) was used for supplying feed water to the evaporator with duty point of 3 m head at 180 kg/s discharge rate. The power rating of the pump is around 9 kW. The specific electrical consumption of the feed pump due to high seawater pressure required by the nozzle was reduced by the vacuum maintained inside the evaporator. This vacuum lowered the injection pressure required by the feed pump by sucking the feed water from de-aerator through nozzles. Moreover, the entire flow rate of feed water was equally shared by 21 nozzles out of 24 nozzles that resulted in reduced flow velocity in each nozzle and hence the pressure loss. It was observed during plant operation that at least three nozzles placed closed to the evaporator shell were unable to splash water properly. The injection pressure in the nozzles was found to be around 0.17 bar (approx.). For circulating the deep sea cooling water inside the cupro-nickel tubes of the condenser, the submersible type seawater pump was used whose pumping head is slightly higher than the feed water pump head by 3 m so that total pumping head comes to 5 m at a pumping capacity of around 150 kg/s. The pumping power consumption was reduced to 13 kW after taking the advantage of the siphoning effect in the cooling water circuit, since both the pipeline ends were immersed below the liquid surface.

3. Determining the flash evaporation rate and evaporation ratio inside evaporator

3.1. Evaporation rate

According to the heat balance equation, the heat lost by the warm feed water is equal to the latent heat gained by the evaporating vapour from the water.

For the given feed water flow rate and the saturation pressure, the mass of vapour generation as a result of flashing can be obtained by the following model using super heat Muthunayagam et al. [9]:

$$M_f\ C_p\ \Delta T_{sup} - M_v\ h_{fg} = 0 \tag{1}$$

$$\therefore M_v = \frac{M_f\ C_p\ \Delta T_{sup}}{h_{fg}} \tag{2}$$

Terms such as conduction, convection and radiation were not included in the Eq. (2). Also the heat loss that occurred through the shell of the evaporator was neglected, since its effect on evaporation rate is negligible. The above equation was formulated based on the fact that all the sensible heat content of the feed water above the saturation temperature corresponding to the saturation pressure of the evaporator was completely utilized for vaporization, such that temperature of the brine liquid reaches that saturation temperature which is denoted by the ΔT_{sup}, super heat.

The relationship between T_{sat}, super heat ($T_{wi} - T_{sat}$) and warm feed water flow rate (M_f) can be obtained from the energy balance equation (Eq. (2)). In the present study, it was observed that with increase in mass flow rate of feed water (M_f), the vapour generation rate (M_v) was found to be increased with corresponding increase in T_{sat} and superheat values. By applying the above observations to the Eq. (2), the theoretical vapour generation rate, M_v was found out which showed an increasing trend similar to the results observed in the experimental study, but with slightly higher value. From the experimental study, it was observed that the saturation pressure could not

be maintained constant or even reduced, when the mass flow rate of feed water was increased (M_f).

Similarly, the same observed process parameters were applied to the below-mentioned Eq. (3) proposed by A.K. El-Fiqi et al. [10] (which was developed based on actual heat) and results were recorded:

$$M_f\ C_p\ T_{wi} - M_f\ C_p\ T_{wo} - M_v\, h_{fg} = 0 \tag{3}$$

The results showed that an increasing trend of vapour generation rate was obtained as observed in the experimental study, but with slightly lower values. The reasons for the variation in the results of both the equation with the experimental values were investigated and presented in this paper.

3.2. Evaporation ratio or yield ratio

The evaporation ratio gives the percentage of evaporation that was achieved from the given amount of the feed water that was being pumped into the evaporator. The evaporation ratio can be obtained from the following Eq. (4):

$$\frac{M_v}{M_f} = \frac{C_p\ \Delta T_{sup}}{h_{fg}} \tag{4}$$

where M_v—mass flow rate of vapour generation (kg/s), M_f—mass flow rate of feed water (kg/s), C_p—specific heat capacity of feed water (kJ/kg K), ΔT_{sup}—superheat (K) ($T_{wi} - T_{sat}$), h_{fg}—latent heat of evaporation (kJ/kg).

3.3. Superheat of the liquid

The superheat of the liquid is the difference in temperature between the saturation point and the warm feed water at the inlet of the evaporator. Increase in the superheat results in the increase in evaporation rate. Therefore, the superheat can be considered as the driving force for enhancing the evaporation rate:

$$\Delta T_{sup} = T_{wi} - T_{sat} \tag{5}$$

where T_{sat}—saturation temperature of evaporator (K), T_{wi}—inlet temperature of feed water (K).

3.4. Actual heat of the feed water

The actual temperature difference between the inlet feed water and the outlet brine discharge coming out of the evaporator is the actual heat of feed water, which is shown below:

$$\Delta T_{actual} = T_{wi} - T_{wo} \tag{6}$$

where T_{wi}—inlet temperature of feed water (K), T_{wo}—outlet temperature of feed water (K).

This difference in temperature is due to the drop in sensible heat of feed water as a result of the flash evaporation inside evaporator.

3.5. Flashing efficiency of the evaporator

Since all feed water entering the evaporator did not lose temperature completely and it depends on flow rate as well as the residence time of feed water exposed to the vacuum zone and also the liquid level maintained inside the evaporator. Flashing efficiency is defined as follows:

$$\eta = \frac{\Delta T_{actual}}{\Delta T_{sup}} = \frac{(T_{wi} - T_{wo})}{(T_{wi} - T_{sat})} \tag{7}$$

where ΔT_{actual} represents the actual evaporation happens inside evaporator and ΔT_{sup} represents the maximum evaporation possible inside evaporator for that feed water flow with respect to the saturation temperature.

3.6. Non-equilibrium temperature difference [NETD] or thermal loss

It is the difference in temperature between the brine discharge outlet and the saturation temperature of the evaporator. For attaining the equilibrium condition as result of the flash evaporation, the temperature of the evaporated brine water should reach the saturation temperature corresponding to the saturation pressure maintained inside the evaporator. NETD can be estimated as follows:

$$\text{NETD} = T_{wo} - T_{sat} \tag{8}$$

where T_{sat}—saturation temperature (K), T_{wo}—brine discharge outlet water temperature (K).

4. Results and discussions

4.1. Effect of feed water nozzle geometry on following parameters

4.1.1. Non-equilibrium temperature difference (NETD) or thermal loss

The objective of this study was to minimize the thermal loss incurring in the flashing process and to

improve the flashing rate that were taking place in the LTTD desalination process. In order to achieve this, two different geometries of spout nozzles such as 0.37–0.87 m with the diameter of 0.1–0.25 m, respectively, were employed in the experiment. Initially 0.37 m height and 0.1 m diameter nozzle was experimented for feed water flow rates that gradually increased from 110 to 190 kg/s and corresponding value of NETD ($T_{wo} - T_{sat}$) was recorded and plotted in Fig. 5. The Fig. 5 depicted that the NETD showed a decreasing trend from 4.1 to 2.8°C as the feed water flow rate increased gradually inside the evaporator. But, when the nozzle height was increased from 0.37 to 0.87 m, the NETD was found to be varying between 3.51 and 1.9°C for the same feed water flow rate (Fig. 5). These experiments indicated that the NETD was decreased by 0.7°C average when 0.87 m height nozzle was implemented (Fig. 2). This could be due to the fact that when the nozzle height was increased by 0.5 m, the residence time of the splashed water exposed to vacuum zone was increased (Fig. 6) that in turn increase the possibility of more latent heat to be released from the feed water resulted in the decreased NETD compared to 0.37 m nozzle, where the residence time of the splashed water would be comparatively lesser than 0.87 m (Fig. 6). Because of this short residence time, the unevaporated feed water would have fallen quickly and mixed with the brine discharge water before losing its sensible heat fully for vapour conversion. It was noted in the experiment that at maximum feed water flow rate, the NETD showed a least value which could be due to the increased jet height of splashed water from the nozzle as a result of increased exit velocity for the corresponding increase in the feed water flow rate. As the jet velocity increased, the residence time of feed water

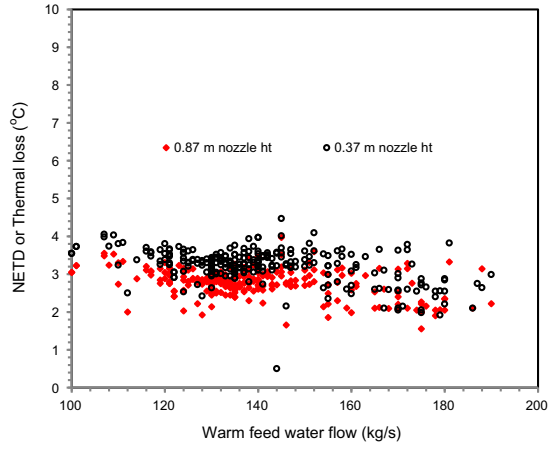

Fig. 5. M_f vs. NETD.

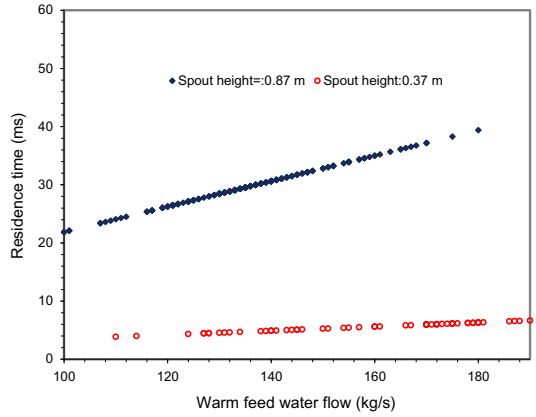

Fig. 6. M_f vs. residence time.

in vacuum zone was also increased. But it was reported in the literature that increased jet height would increase the local liquid pressure as a result of increased water column height [11]. This would delay the evaporation to initiate, but the implementation of the 0.25 m diameter nozzle at the nozzle tip would reduce the water jet height to a certain extent that may reduce the delay in initiation of the evaporation of feed water and maximize the surface area exposed to the vacuum zone resulted in increased flashing rate.

Drawbacks of 0.37 m nozzle height compared to 0.87 m nozzle are discussed below:

(1) Insufficient residence time that resulted in increased NETD or thermal loss.
(2) No splashing of feed water from the nozzles during high tide, which resulted in pool evaporation. This was because of the nozzle that was completely submerged below the brine discharge liquid level during high tide inside evaporator.
(3) This lead to decreased evaporation rate and increased NETD.

Some of the suggestions to minimize the NETD or thermal loss in the LTTD process are as follows:

(1) Enhancer such as spray nozzles can be employed for splashing the sea water that would increase the surface area of water exposed to vacuum.
(2) Increase in the residence time travel of feed water inside the evaporator would reduce the thermal loss to a certain extent.
(3) Improper selection of nozzle size may some time lead to increased pressure drop and

power consumption of the feed pump. Therefore, care should be taken, when selecting the nozzle size for the flashing process.

(4) Arrangement of nozzle pattern inside the evaporator also had influence on the NETD.
(5) Improper arrangement of nozzle inside evaporator may result in uneven distribution of water in the nozzles. This would lead to a situation in which some portion of the evaporator was left with no feed water at all, especially in the nozzles that were located closer to the evaporator shell that resulted in increased nozzle pressure drop and reduced flashing efficiency. This in turn increases the NETD value.
(6) Maintaining of low brine discharge liquid level inside the evaporator would reduce the NETD by maximizing the feed water droplet travelling time before mixing up with brine liquid.
(7) Increase in the nozzle height would improve the release rate of latent heat from feed water which in turn reduced the approach temperature between the feed outlet water (T_{wo}) and the saturation temperature (T_{sat}), thus minimizes the NETD. Vacuum maintained at the tip of the nozzle support the water column height in the extended nozzles provided no appreciable increase in static head of the feed pump.

4.1.2. Flash evaporation processes

As discussed in the previous section that the increase in the spout nozzle height resulted in the decrease in NETD which in turn increases the flashing rate, since the reduced NETD meant that increased temperature drop in the feed water towards the saturation temperature. This indicated that more amount of the heat was released from the feed water for generation of water vapour. The results were depicted in the Fig. 7 which showed that an increase in the feed water flow rate (M_f) resulted in an increase in the vapour generation rate (M_v) for the two different nozzle geometry of 0.37–0.87 m. This Fig. 7 also indicated that when the nozzle height was increased from 0.37 to 0.87 m the vapour generation rate was found to be increased by 0.9% average. In the present study, the superheat of the liquid varied between 4 and 5°C only with feed water temperature of around 29.9°C maximum available at the surface layers of the sea during the experiment. The saturation temperature maintained in the evaporator would be in the range of 25–26°C and cooling water temperature was in the range of 12–13°C only. The nozzles employed in the present study was provided with small concentric disk

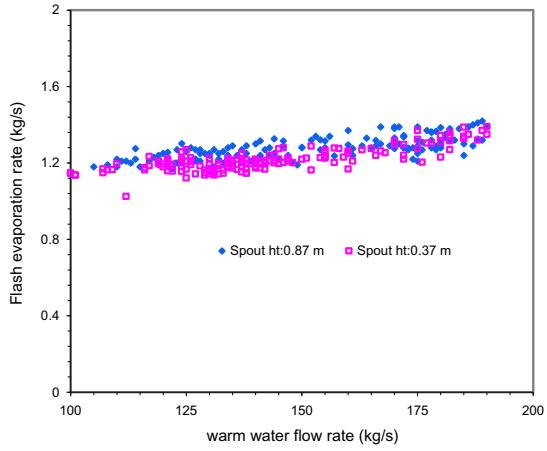

Fig. 7. M_f vs. M_v.

at the mid portion. This would be helpful in scattering the water jet in to a small particle, so that the flash evaporation would be enhanced to a certain amount. Enough clearance was provided between disk and nozzle inner diameter through which water jet ejected out after hitting the disk resulted in the formation of scattered water spray to minimize the droplet thickness and maximize the flash evaporation rate. No appreciable increase in the feed water pump head was observed when these small concentric disks were used in the nozzles.

Some of the suggestions to enhance the evaporation rate in the LTTD process are as follows:

(1) Increasing the residence time of the water jet coming out from the nozzle would certainly increases the flash evaporation rate.
(2) Putting of small hindrance without affecting the flow of liquid jet in the nozzle could decrease the spray thickness which might be helpful in increasing the evaporation rate.
(3) Increasing the height of the nozzle increases the evaporation rate and also it avoids the submergence of the nozzle below the brine discharge liquid level during the high tide period.
(4) Space provided between adjacent nozzles, i.e. pitch of the nozzles may also have influence on the flashing process since equalized spacing of nozzles with respect to the given evaporator size would utilize the available flashing area to a maximum for the flash evaporation enhancment.
(5) Placing of nozzles closer to the evaporator shell should be avoided, as these nozzles might be starving for the water jet to form due to uneven water distribution.

4.2. Investigation of effect of process parameters on the liquid flashing in LTTD process

4.2.1. Effect of warm feed water flow rate on liquid flash evaporation and other process parameters (0.87 m nozzle)

Experiments were conducted for different warm feed water flow rates and corresponding mass of vapour generated in evaporator were measured by condensing the vapour in the shell and tube condenser. Evaporation rate based on the actual heat, i.e. temperature drop of the feed water ($T_{wi} - T_{wo}$) was predicted using the correlation given in Eq. (3). Similarly, the evaporation rate estimated based on the super heat ($T_{wi} - T_{sat}$) corresponding to the saturation temperature of evaporator was predicted using the model given in Eq. (2). Comparison plot of both the predictions with the measured evaporation is shown in the Fig. 1. The above Fig. 8 depicted that increase in feed water flow rate increased the evaporation rate. Also, it was observed that the evaporation rate determined based on super heat corresponding to the given feed water flow rate over predicted the measured evaporation rate that occurred inside the evaporator. On the other hand, evaporation rate predicted based on the actual heat ($T_{wi} - T_{wo}$) matched closer to the evaporation rate measured with 20% deviation maximum and 5% deviation minimum. The Fig. 9 depicted that when the feed water flow rate was increased, the super heat of the liquid was found to be decreased and saturation pressure was found to be increased, as all these parameters were related (i.e. dependent) to each other. As more quantity of water vapour was released from the seawater, the evaporator pressure was increased gradually, this in turn increased the saturation temperature that lead to reduced superheat.

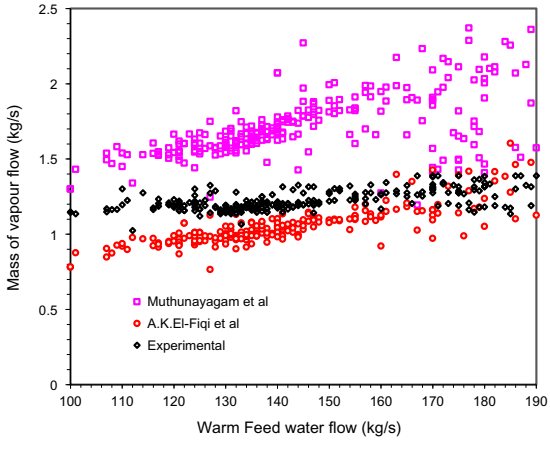

Fig. 8. M_f vs. M_v.

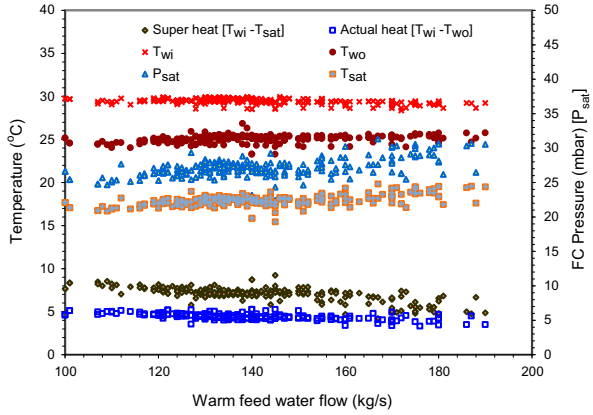

Fig. 9. M_f vs. temp.

Since the parameters such as T_{sat}, superheat ($T_{wi} - T_{sat}$) and feed water flow rate (M_f) were dependent on each other, any increase in the feed water flow rate found to be having an adverse effect on the other parameters such as increase in T_{sat}, decrease in superheat and the positive effect on the vapour generation rate. Increased pressure in the evaporator could be due to the restriction in the flow of vapour through a small vapour duct that connects the evaporator to the condenser. Increased mass flow rate of vapour resulted in increased friction in the vapour duct that would restrict the free movement of water vapour. This in turn led to increased local pressure of the evaporator.

Fig. 9 shows that the drop in temperature of feed water was observed across the evaporator as the feed water flow rate was increased. At low feed rate of around 100 kg/s the drop in temperature was around 5.5℃ but, when the feed water flow rate was increased to 190 kg/s the temperature drop was decreased to 3.8℃. It was also observed from the Fig. 9 that as the feed water flow rate increased, the parameters such as brine liquid temperature (T_{wo}), saturation pressure (P_{sat}), saturation temperature (T_{sat}) increased, except NETD ($T_{wo} - T_{sat}$) or thermal loss, which showed a decreasing trend. It was observed that the feed water inlet temperature (T_{wi}) was varied to a maximum of 1℃ during the experiment that was due to change in sea condition.

Fig. 10 indicates the percentage of variation in the calculated evaporation rate compared to the measured evaporation rate. The curve which showed an upward trend represents the deviation of evaporation rate obtained based on the superheat of liquid ($T_{wi} - T_{sat}$) with respect to the feed water flow rate (M_f). This percentage of deviation keep on increasing as the flow rate of feed water was increased gradually. Possible

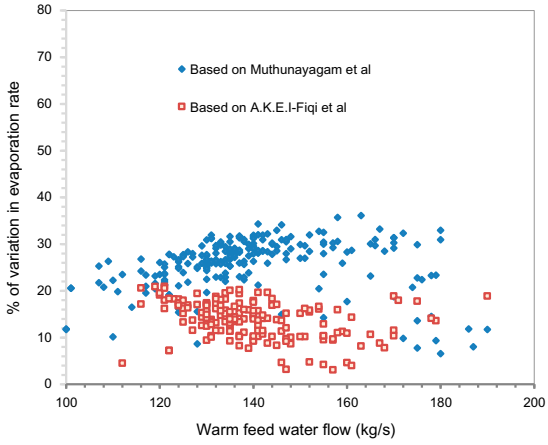

Fig. 10. M_f vs. % variation in M_v.

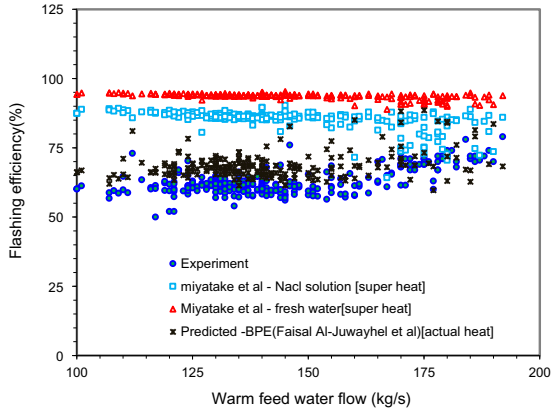

Fig. 11. M_f vs. η.

reason could be due to the parallel increase in the saturation temperature of evaporator with mass flow rate of feed water. This percentage of deviation varied from 20 to 35% for the feed water flow rate that varied between 100 and 190 kg/s. Amount of deviation was not consistent because drop in super heat of water showed downward trend with respect to the increase in feed water flow rate (Fig. 9). However, evaporation rate calculated based on actual heat ($T_{wi} - T_{wo}$) showed a reduction in percentage of deviation with measured evaporation rate in the range below 20% and this deviation still decreased and reached closer to the experimental value up to 5% when maximum feed water flow rate was maintained in the evaporator.

It was noted that there were two factors that lead to more percentage of deviation to occur for the super heat compared to actual heat were, the slope of the trend in the curve for super heat was more than the actual heat as shown in Fig. 9 for the same feed water flow rate and drop in inlet temperature of feed water as a cause of seasonal variation during the experiment (Fig. 9). It was observed during the experiment that at maximum feed water flow rate, the difference of temperature between the superheat and actual heat decreases that certainly started to happen above 170 kg/s feed rate. This event attributed to the increase in flashing efficiency specifically after 170 kg/s feed rate. Fig. 11 depicts that the points initially showed a constant trend and later it showed an increasing trend. This curve pattern was obtained as the saturation temperature corresponding to the measured evaporator pressure was increased with respect to mass flow rate of feed water with parallel decrease in feed water inlet temperature. Also, it was observed that the variation in the warm feed water inlet temperature and super heat for different warm feed water flow rates followed same trend pattern as shown in Fig. 9. These two measured parameters have combined effect on the flashing efficiency that showed an increasing trend after 170 kg/s feed water rate (Fig. 9). Predicted efficiency during the design stage calculated based on the thermal loss due to BPE using correlation suggested by Faisal Al-Juwayhel et al. [12] was also compared with experimental results. Predicted efficiency was determined based on the calculated BPE with respect to warm water inlet temperature. Fig. 11 clearly indicated that the predicted efficiency was moderately greater than the experimental value. Since the thermal loss or NETD in predicted efficiency was calculated as 0.7°C due to BPE as a result of salt impurities, whereas the actual measured thermal loss inside evaporator was in the range of 1.9–3.51°C ($T_{wo} - T_{sat}$) (Fig. 12). This resulted in decreased flash efficiency in the experiment than the calculated value. This could be due to insufficient residence time available for the feed water inside the evaporator to undergo vaporization. This could be controlled to certain extent by increasing the spout nozzle height further above 0.87 m, but this may have penalty on the water quality and pump head marginally. Miyatake et al. [13] formulated two correlations for Nacl solution and water for estimating the flash efficiency which were used for comparison with present experimental results as shown in Fig. 11. Flash efficiency determined using Eqs. (9) and (10) for Nacl solution and fresh water, respectively, over predicted the experimental value. Because this equation did not consider the parameter such as variation in the feed water flow rate that decided the evaporation rate and efficiency in the experiment.

Effect of feed warm water flow rate (M_f) on the evaporation ratio (i.e. percentage of evaporation rate

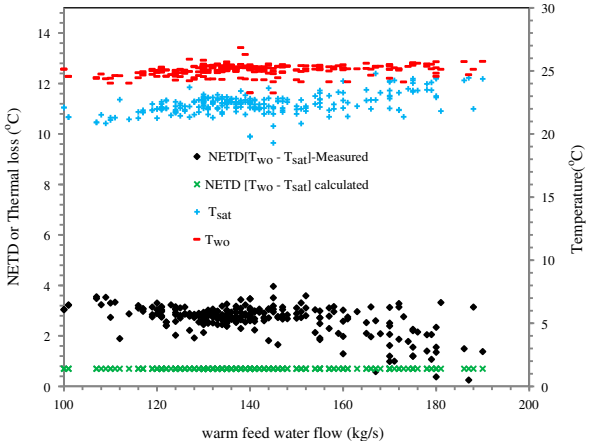

Fig. 12. M_f vs. NETD.

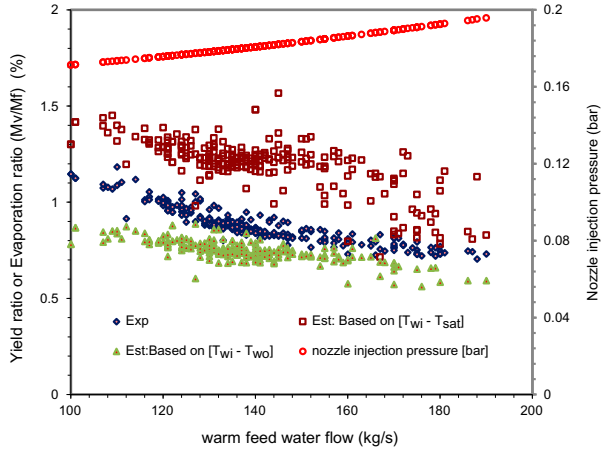

Fig. 13. M_f vs. (M_v/M_f).

with respect to corresponding feed water flow rate) was shown in Fig. 13. The figure indicated three different curves plotted for different feed water flow rates. Top curve was drawn based on the super heat of water which showed highest amount of evaporation ratio obtained for the corresponding given feed water flow rate that varied between 1.42 and 0.8% decreased with increase in the feed water flow rate. Top curve actually over predicted the measured evaporation ratio. Bottom curve was obtained based on the estimation with the actual heat ($T_{wi} - T_{wo}$) measured in the evaporator which showed value between 0.9% maximum and 0.6% minimum corresponding to the measured feed water flow rate. This clearly indicated that the evaporation ratio was under predicted in this case. But the middle curve showed the evaporation ratio that varied between 0.7 and 1.12%, which was estimated based on the measured vapour generation rate as well as feed rate. This maximum value of 1.12% yield ratio was obtained corresponding to the nozzle injection pressure of around 0.17 bar (approx.) after taking into the account the vertical height of nozzle (1.6 m) and friction loss inside nozzles due to the flow velocity. It was observed during the experiment that at least 90% of the nozzles were fully engaged in the water splashing inside the evaporator. Variation in nozzle injection pressure with respect to the feed water flow rate was depicted in Fig. 13. Over prediction of evaporation ratio calculated based on super heat ($T_{wi} - T_{sat}$) could be due to the measured saturation pressure (P_{sat}) which might be differing from the actual evaporation pressure near the flashing zone which was unknown. Since the measurements were taken near the shell of the evaporator whereas the actual flash evaporation occurs in the middle of evaporator that too even near the mouth of the spout where flashing actually occurs. Pressure could be more in the actual zone of evaporation than the measured pressure (P_{sat}) near shell walls. This would lead to over prediction of evaporation ratio using super heat compared to evaporation ratio calculated based on the actual evaporation rate, since the T_{sat} for superheat was obtained from the measured P_{sat}. In the other case, the evaporation ratio calculated using actual heat ($T_{wi} - T_{wo}$) was under predicted because of the outlet brine discharge liquid temperature (T_{wo}) that was a mixed temperature of both evaporated and unevaporated feed water. The temperature of the unevaporated water would be higher than the evaporated water. The feed water enters and leaves the evaporator with a short residence time. Sufficient time might not be available for the outlet liquid for proper mixing; as a result, the temperature of brine liquid might be differing from the actual temperature. This could lead to under prediction of evaporation ratio by actual heat.

As discussed already, when the mass flow rate of feed water was increased, the evaporation ratio showed a decreasing trend. This was due to the fact that the percentage of vapour generation rate at low feed water flow rate was higher due to low operating pressure compared to the vapour generation rate that was taking place at high feed water flow rate with high operating pressure. For better understanding, it was explained in the following way using the measured data, i.e. for 100 kg/s (M_f) feed rate, the evaporation rate was measured as 1.12 kg/s (M_v), but when the feed water flow rate was increased to 190 kg/s (M_f) the evaporation rate was measured as 1.34 kg/s (M_v). This showed that the evaporation ratio ((M_v/M_f) × 100) at low feed rate was 1.12% but at high feed rate it was only 0.7%. But if we compare the

vapour generation rate measured at two extreme flow rates of feed water, it was found that the vapour generation rate was maximum only at high feed water flow rate. This could be because of the raise in saturation pressure that allowed only a small increment in vapour generation rate for every increment in the feed water flow that entered the evaporator which resulted in reduced evaporation ratio at high feed water flow rates.

4.2.2. Influence of evaporator pressure on flash evaporation and other process parameters (0.87 m nozzle)

The evaporator pressure was increased when ever the amount of vapour generation inside evaporator was increased, as a result of entry of more amount of feed water in to the evaporator. Fig. 14 depictes that at a low evaporator pressure, the amount of heat generated due to vaporization was found to be less for the given feed water water flow rate. Eventhough, the amount of drop in feed water temperature was more, still the quanity of vapour generated was less at low evaporator pressure when compared to high evaporator pressure dominated by high feed water flow rate. However, the quanity of water needed for evaporation was comparatively higher at high evaporator pressure for getting a small increment in vapour generation rate compared to vapour generation at low feed water flow rate. It was noticed that during the experiment that at high feed water flow rate, the reduction in evaporator pressure could not be achieved.

Top curve in Fig. 14 clearly shows that the heat load estimated based on the latent heat of vaporization corresponding to the measured saturation pressure was greater than the heat load obtained from calculation based on temperature drop of feed water (actual heat). As discussed earlier, this could be due to difference in the transmitter measured pressure (fitted in the shell wall away from the flashing zone) and the saturation pressure prevailing in the actual flashing zone as discussed earlier.

Fig. 15 indicates that at high evaporator pressure, the experimental mass flow rate of vapour generated showed an increasing trend when the evaporator reached 28 m bar pressure due to increased mass flow rate of feed water. Similar trend was observed for mass of vapour generated based on measured actual heat. But decline trend was observed for mass of vapour generation predicted based on super heat with raise in saturation pressure inside evaporator. As the pressure increased, the corresponding saturation temperature was also increased that lead to a reduction in the super heat available inside evaporator. Curve plotted for predicted mass of vapour generation based on actual heat matched closer with the curve of measured mass of vapour generated. NETD and actual heat showed decreasing trend with increase in evaporator pressure. Since the increase in saturation pressure shifted the saturation temperature closer to the feed water inlet temperature. As a result, the drop in temperature of feed water decreases that certainly lead to a decreased NETD or thermal loss as well as actual heat.

Actual evaporation depends on the factors such as saturation pressure, flow rate of feed water, height of spout nozzle above the brine discharge liquid, the residence time of liquid exposed to low pressure zone and height of jet coming out of spout nozzle mouth. If sufficient residence time was provided for the water that enters the evaporator, then the actual heat could be increased to a certain extent. However, the

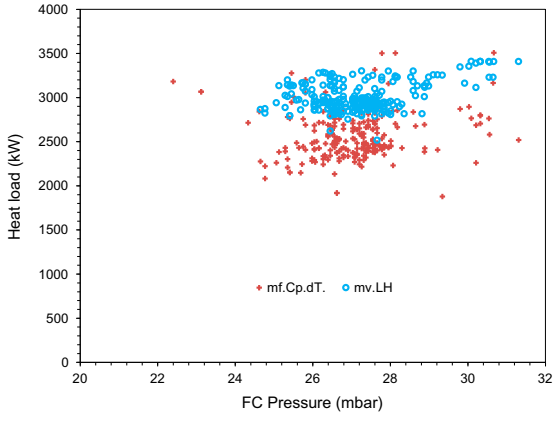

Fig. 14. P_{sat} vs. Q.

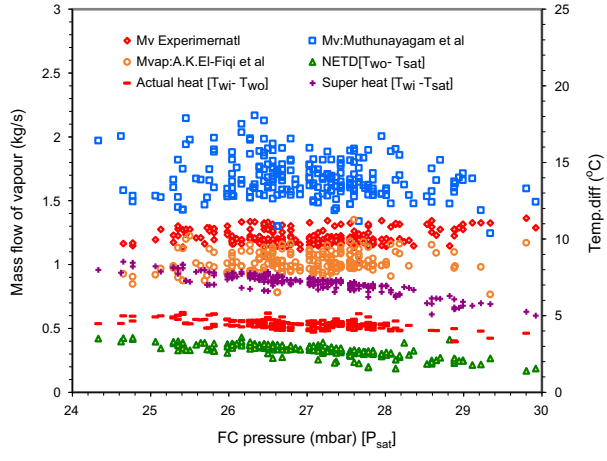

Fig. 15. P_{sat} vs. M_v and ΔT.

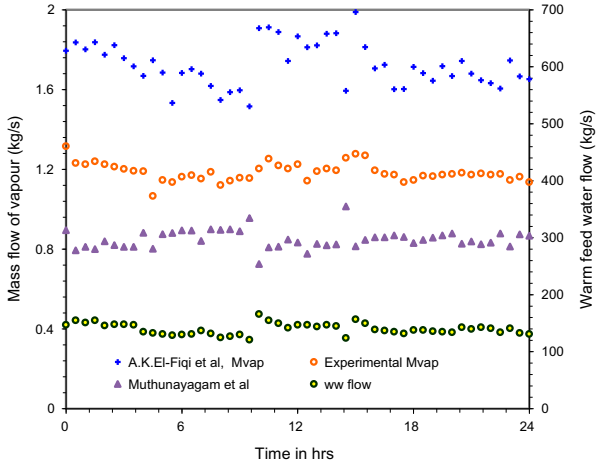

Fig. 16. Time vs. variation in M_v, M_f.

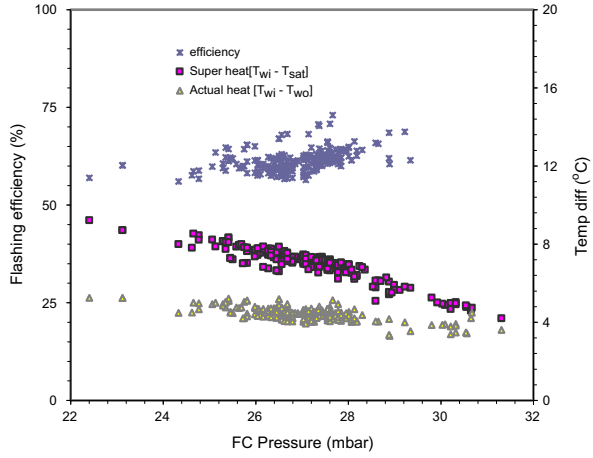

Fig. 18. P_{sat} vs. η and ΔT.

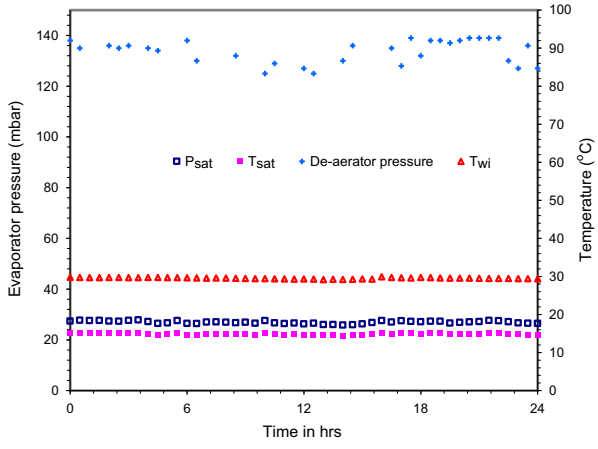

Fig. 17. Time vs. variation in process parameters.

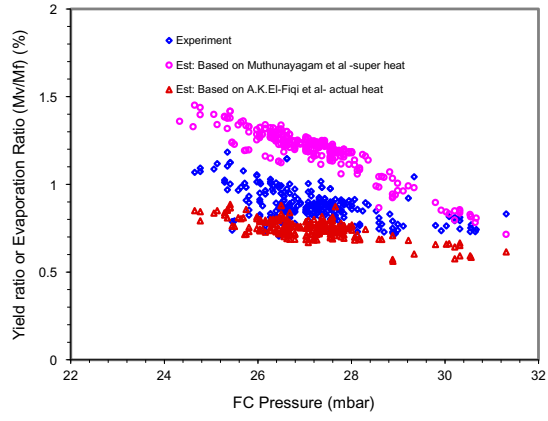

Fig. 19. P_{sat} vs. M_v/M_f.

presence of salt impurity in the seawater lead to an increase in the BPE that would create certain amount of thermal losses that resulted in reduced super heat and actual heat marginally. Flooding height inside evaporator reduces the residence period. The variation in the process parameters with respect to time is shown in Figs. 16 and 17. Fig. 18 indicates that the increase in efficiency due to increase in feed water flow rate was observed at high evaporator pressure; because, the drop in super heat was comparably higher than drop in actual heat, since efficiency is the ratio of actual heat to the super heat. This was evident from the slope of curve which is depicted in the Fig. 18, where the slope of the superheat was steeper than slope of actual heat for the same evaporator pressure.

Evaporation ratio from the given amount of feed water rate was found to be higher during low evaporator pressure as indicated in Fig. 19 and at low feed water flow rate (Fig. 13). For example at 100 kg/s feed water flow rate, the experimental vapour generation rate was around 1.12 kg/s. Predicted generation rate was 1.31 kg/s with respect to super heat measured for that flow rate. Similarly for actual heat, the corresponding predicted vapour generation rate was around 0.75 kg/s. When the feed water flow rate was reached to 190 kg/s, the experimental value increased to 1.34 kg/s, the predicted value based on super heat reached to 2 kg/s and predicted value based on actual heat increased to 1.12 kg/s. Evaporation ratio was increased as the evaporator pressure and feed water flow rate was decreased, but evaporation rate was increased when the feed water flow rate was increased.

4.2.3. Super heat of working fluid (seawater) inside evaporator ($T_{wi} - T_{sat}$) (0.87 m nozzle)

It was depicted in Fig. 20 that the feed water flow rate showed a decreasing trend with an increased super heat value. Similarly, the above figure depicted that predicted vapour generation rate based on actual heat showed a decreasing trend with decrease in feed water flow rate. But the prediction of vapour generation rate based on the super heat projected a reverse trend. Measured vapour generation rate (i.e. experimental) corresponding to super heat of the liquid measured showed a declining trend similar one to actual heat. Reverse trend of the super heat was due to pressure difference between actual zone of evaporation and location of pressure transmitter. Actual measured evaporation rate depends on flashing pressure at the zone where the feed water was being flashed from the mouth of spout nozzle as discussed earlier.

Miyatake et al. [13] proposed an empirical formula for estimating flashing efficiency for an aqueous NaCl solution (Eq. (9)) and water (Eq. (10)). These empirical formulae were independent of velocity of water from nozzle, equilibrium or flash chamber temperature, length and diameter of nozzle. The formulae are given as follows:

$$\eta_{\text{flashing}} = 1 - [1 + 1.5 \times (\Delta T_{\text{sup}} - 3.0)]^{-1} \quad (9)$$

$$\eta_{\text{flashing}} = 1 - [1 + 2.5 \times (\Delta T_{\text{sup}} - 1.0)]^{-1} \quad (10)$$

where ΔT_{sup} is super heat of liquid in K.

The above Fig. 21 depictes that the flashing efficiency was calculated using formula suggested by Miyatake et al. [12] showed an increasing trend with

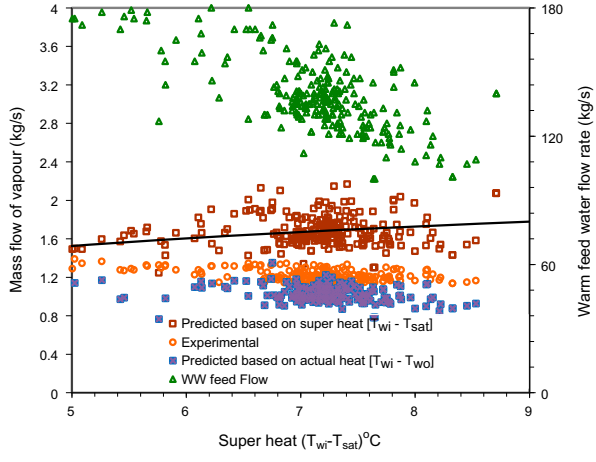

Fig. 20. ΔT_{sup} vs. M_{v}, M_{f}.

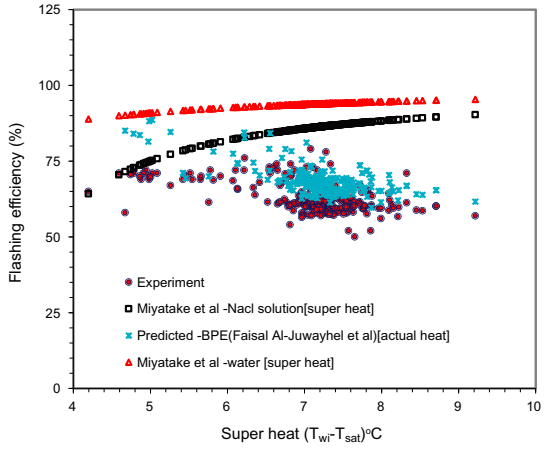

Fig. 21. ΔT_{sup} vs. η, temp.

respect to increase in super heat. This formula did not include the effect of the feed water flow rate variation where the feed water flow rate was declined continuously with every increase in super heat and did not remain constant in the present work. Miyatake et al. [13] conducted experiments at different super heats by varying the pressure and temperature but at constant feed water flow rate. However, in the present work the flows have been subjected to fluctuations due to variation in tide level of ocean. Increase in tide level, increased the feed water flow rate that proportionately increased the evaporator pressure, which in turn decreased the super heat. The flash efficiency predicted during design stage based on the thermal loss due to BPE was depicted in the Fig. 21. BPE was calculated to be around 0.7°C. The fig indicated that the predicted efficiency based on BPE was found to be greater than the experimental flash efficiency. Predicted efficiency based on Miyatake et al. correlation indicated an increasing trend with increase is super heat value. This could be because of the non-consideration of feed water flow rate in the equation as discussed earlier that lead to increasing trend as opposite to the curve trend obtained for experimental and predicated one using BPE.

4.2.4. Actual heat of feed water inside evaporator ($T_{wi} - T_{wo}$) (0.87 m nozzle)

Difference in temperature between inlet feed water and outlet brine discharge water was termed as actual heat of evaporator, i.e. the drop in temperature of feed water across evaporator. It was clearly indicated in the Fig. 22 that as the actual heat increased; the evaporation ratio obtained from the experiment showed an increasing trend which was closer to the evaporation

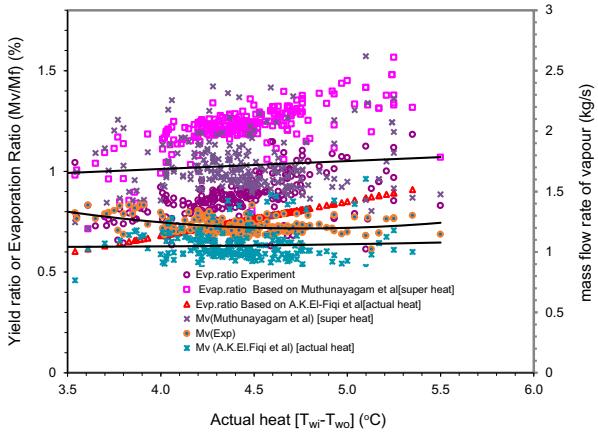

Fig. 22. ΔT_{actual} vs. M_v/M_f, M_v.

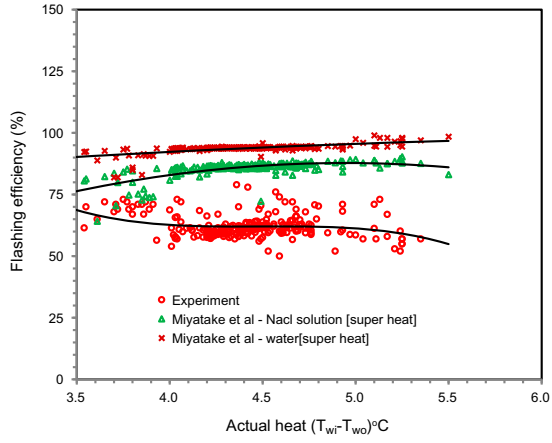

Fig. 23. ΔT_{actual} vs. η.

ratio predicted corresponding to the observed actual heat. Evaporation ratio estimated based on super heat over predicted the measured evaporation ratio. At 3.5°C temperature drop of feed water (i.e. actual heat), the experimental evaporation ratio comes to 0.76%, predicted evaporation ratio based on actual heat comes to 0.60% and predicted evaporation ratio obtained based on the super heat comes to 0.84%.

When the temperature drop, i.e. the actual heat was increased further up to 5°C the corresponding evaporation ratio was increased to 0.99, 0.80 and 1.36% for experimental, actual heat and super heat, respectively. It was observed that at the low temperature drop, the deviation in the evaporation ratio was less, but as the drop in temperature of inlet feed water inside evaporator was increased due to vaporization, the deviation in evaporation ratio between the experimental and calculated evaporation ratio based on the actual heat also found to be increased (Fig. 22). Also the figure depicted that at a low temperature drop of feed water, the measured mass of vapour generation was found to be more and the trend showed decrement in the vapour mass flow for further increment in the temperature drop, i.e. actual heat. But the calculated mass of vapour generation rate obtained based on superheat showed increasing trend and actual heat showed a horizontal trend. This increasing trend in super heat could be due to the measured saturation pressure using transmitter might be lesser than the pressure that was prevailing at the actual zone of evaporation which was already discussed. It was depicted in the Fig. 23 that the increase in actual heat resulted in the increase in flashing efficiency estimated based on superheat that varied between 87 and 94% for water and for Nacl solution it was varying between 81 and 92% compared to the experimental flashing efficiency calculated based on measured super heat and actual heat. It was observed from the Fig. 23, that at low actual heat value the experimental flash efficiency was found to be higher about 70%, but as the actual heat value was increased the efficiency dropped to 55% minimum. This could be due to the fact that the difference in temperature between super heat and actual heat increased as the actual heat increased. This was because of the increase in saturation pressure (Fig. 18) as a result of increase in feed water flow rate (Fig. 9).

5. Concluding remarks

An experimental study was carried out to find the effect of feed water nozzles on NETD and flash evaporation and observed results were discussed below:

(1) Two different spout nozzle geometries with 0.37–0.87 m height were employed in the experiment.
(2) The study indicated that when the nozzle height was increased from 0.37 to 0.87 m the corresponding flashing rate was increased by 0.9% (average) and and the NETD ($T_{wo} - T_{sat}$) was decreased by 0.7°C (average).
(3) This was due to increased flashing surface area, residence time and decreased thickness of the water sprayed with disk plates fitted in nozzle for scattering the feed water.
(4) Decrease in flood level inside evaporator resulted in increased travelling time of the water particle exposed to vacuum before mixing up with the brine discharge water lead to an increased flashing efficiency and decreased NETD value.

(5) Increase in tide level flooded the 0.37 m height spout nozzle resulted in non-splashing of feed water. This in turn lead to decreased flash evaporation and increased NETD or thermal loss.
(6) Variation in tide level did not flood the nozzle when its height was increased up to 0.87 m. Splashing of water was taking place without any disturbance resulted in increased flashing efficiency and reduced losses.

Following observations were made from the investigation that was carried out to find the effect of process parameters on liquid flashing for 0.87 m height nozzle configuration:

(1) Experimental study indicated that the operating parameters of the evaporator such as saturation pressure (P_{sat}), saturation temperature (T_{sat}), superheat ($T_{wi} - T_{sat}$), outlet temperature of brine discharge water (T_{wo}) and mass of vapour generation (M_f) were influenced by the amount of feed water (M_f) that were pumped into the evaporator.
(2) It was reported in literature that 4% yield ratio was obtained for a nozzle injection pressure of 1 bar for a similar desalination process. But in the present study, a maximum of 1.12% yield ratio was obtained with a nozzle injection pressure of around 0.17 bar.
(3) In order to fine tune the evaporator design for future LTTD plants, the experimental results of flash evaporation were compared with two mathematical models obtained from the literature. While comparing the results, it was observed that the model which used actual heat ($T_{wi} - T_{wo}$) made a good agreement with the experimental data compared to the other model that used superheat ($T_{wi} - T_{sat}$). This could be because of difference in saturation pressure between the measured one using transmitter near to the wall and the pressure at the actual zone of evaporation which might be higher than the measured pressure.
(4) Increased vapour generation rate was observed with increased feed water flow rate, which in turn lead to increased saturation pressure and reduced superheat. This could be due to the fact that the flow restriction experienced by the vapours when they were flowing in hugh quantity through a small vapour duct resulted in increased saturation pressure of the evaporator and hence the saturated temperature. Since the super heat ($T_{wi} - T_{sat}$) was depended on the saturation temperature, the increase in T_{sat} correspondingly decreases the super heat.
(5) It was observed from the experimental study that, when the mass flow rate of feed water was increased, the evaporation ratio showed a decreasing trend. This could be because of raise in pressure that allowed only a small increment in vapour generation rate from the feed water that entered the evaporator which resulted in reduced evaporation ratio at high feed water flow rates. If it was possible to maintain constant saturation pressure inside the evaporator, then the evaporation ratio would have been increased with corresponding increase in mass flow rate of feed water.
(6) This study indicated that improvement in flashing efficiency was observed when the mass flow rate of feed water was increased beyond 170 kg/s and the efficiency was increased from 55 to 75% at high feed water flow rates. This was due to the fact that beyond 170 kg/s, the difference in temperature between actual heat and super heat showed a decreasing trend which resulted in increased flashing efficiency.
(7) It was observed from the experiment that the increase in feed water flow rate up to 11% (190 kg/s) above the design requirement (170 kg/s) resulted in increase in the evaporation rate up to 2.1% above the design value.
(8) Comparison of Miyatake et al. model results with experimental values showed that, with increase in superheat the experimental value showed decreasing trend just opposite to the trend of above said model. This was because of the fact that this model did not include the effect of the feed water flow rate variation which was declined continuously with every increase in super heat and did not remain constant in the present work.
(9) The study indicated that the NETD was found to be varying between 1.9 and 3.51˚C even after increasing the nozzle height from 0.37 to 0.87 m. This was due to insufficient residence time available for vaporization. Further increment in nozzle height could reduce the thermal loss to certain extent, but it may have penatly on the water quality and the pumping head marginally.
(10) Inorder to investigate the possibility of reducing NETD further, it is proposed to continue the experiments by implementing modification in the spout nozzle geometry of the existing evaporator.

Nomenclature

M_f	—	mass flow of feed water (kg/s)
M_v	—	mass flow of water vapour (kg/s)
C_p	—	specific heat capacity of seawater (kJ/kg K)
h_{fg}	—	latent heat of vaporization (kJ/kg)
T_{wi}	—	feed water inlet temperature (K)
T_{wo}	—	feed water outlet temperature (K)
ΔT_{sup}	—	super heat of liquid (K) ($T_{wi} - T_{sat}$)
T_{sat}	—	saturation temperature (K)
ΔT_{actual}	—	actual heat of liquid (K) ($T_{wi} - T_{wo}$)
P_{sat}	—	saturation pressure (m bar)

Symbol

η	—	flashing efficiency of evaporator (%)

Abbrevations

NETD	—	non-equilibrium temperature difference
LTTD	—	low temperature thermal desalination
WW	—	warm water flow
BPE	—	boiling point elevation

References

[1] R.J. Peterson, S.S. Grewal, M.M. El-Wakil, Investigations of liquid flashing and evaporation due to sudden depressurization, Int. J. Heat Mass Transfer 27(2) (1984) 301–310.
[2] O. Miyatake, T. Tomimura, Y. Ide, T. Fujii, An experimental study of spray flash evaporation, Desalination 36 (1981) 113–128.
[3] O. Miyatake, T. Tomimura, Y. Ide, M. Yuda, T. Fujii, Effect of liquid temperature on spray flash evaporation, Desalination 37 (1981) 351–366.
[4] Y. Kitamura, H. Morimitsu, T. Takahashi, Critical superheat for flashing of superheated liquid jets, Ind. Eng. Chem. Fundam. 25(2) (1986) 206–211.
[5] S. Gopalakrishna, V. Purushothaman, N. Lior, An experimental study of flash evaporation from liquid pools, Desalination 65 (1987) 139–151.
[6] O. Miyatake, K. Murakami, Y. Kawata, T. Fujii, Fundamental experiments with flash evaporation, Heat Transfer Jpn. Res. 2(4) (1973) 89–100.
[7] Y. Ikegami, H. Sasaki, T. Gouda, H. Uehara, Experimental study on a spray flash desalination (influence of the direction of injection), Desalination 194(1–3) (2006) 81–89.
[8] R. Brown, J.L. York, Sprays formed by flashing liquid jets, AIChE J. 8(2) (1962) 149–153.
[9] A.E. Muthunayagam, K. Ramamurthi, J.R. Paden, Low temperature flash vaporization for desalination, Desalination 180 (2005) 25–32.
[10] A.K. El-Fiqi, N.H. Ali, H.T. EL-Dessouky, H.S. Fath, M.A. El-Hefni, Flash evaporation in a superheated water liquid jet, Desalination 206 (2007) 311–321.
[11] S. Mutair, Y. Ikegami, Experimental investigation on the characteristics of flash evaporation from superheated water jets for desalination, Desalination 251 (2010) 103–111.
[12] F. Al-Juwayhel, H. El-Dessouky, H. Ettouney, Analysis of single-effect evaporator desalination systems combined with vapor compression heat pumps, Desalination 114 (1997) 253–275.
[13] O. Miyatake, Y. Koito, K. Tagawa, Transient characteristics and performance of a novel desalination system based on heat storage and spray flashing, Desalination 137 (2001) 157–166.